Pain 137 (2008) 574–588

PAIN

www.elsevier.com/locate/pain

Interaction between protein kinase D1 and transient receptor potential V1 in primary sensory neurons is involved in heat hypersensitivity

Haihao Zhu [a,1], Yanrui Yang [a,1], Hua Zhang [b], Yan Han [a], Yafang Li [a], Ying Zhang [a], Dongmin Yin [a], Qihua He [c], Zhiqi Zhao [b], Peter M. Blumberg [d], Jisheng Han [a], Yun Wang [a,*]

[a] *Neuroscience Research Institute & Department of Neurobiology, Key Laboratory for Neuroscience, Peking University, 38 Xueyuan Road, Beijing 100083, PR China*

[b] *Institute of Neurobiology, Fudan University, Shanghai 200433, PR China*

[c] *Healthy Analytical Center, Peking University, PR China*

[d] *Laboratory of Cellular Carcinogenesis and Tumor Promotion, National Cancer Institute, National Institutes of Health, Building 37, Room 4048, 37 Convent Dr., MSC 4255, Bethesda, MD 20892-4255, USA*

Received 16 May 2007; received in revised form 7 September 2007; accepted 22 October 2007

Abstract

In previous studies we demonstrated that protein kinase D1 (PKD1/PKCμ) could directly phosphorylate the transient receptor potential V1 (TRPV1) at its N-terminal region and enhance the function of TRPV1 in CHO cells stably transfected with TRPV1. In the current study we assessed the involvement of PKD1 in pain modulation and explored the possible interaction between PKD1 and TRPV1 in rat inflammatory heat hypersensitivity. PKD1 was translocated to cytoplasmic membrane fraction and was transphosphorylated only in membrane fraction but not in cytoplasmic fraction of dorsal root ganglia (DRG) at 2 and 6 h after Complete Freund's Adjuvant (CFA) treatment. Pre i.t. injection of PKD1 antisense for 4 d or post-i.t. injection for 4 d both alleviated CFA-induced thermal hypersensitivity. Likewise, overexpression of PKD1 in DRG significantly enhanced, while dominant negative PKD1 (DN-PKD1) partly attenuated, heat hypersensitivity. Both PKD1 and TRPV1 were translocated to the cytoplasmic membrane in DRG 6 h after CFA treatment and, at that time, PKD1 interacted with TRPV1 by co-immunoprecipitation in DRG. Electrophysiological measurements indicated that DRG with overexpression of PKD1 were more sensitive to low dose capsaicin than those expressing DN-PKD1. The average magnitude of the peak inward current evoked by capsaicin was greater in the DRG overexpressing PKD1 than in those expressing DN-PKD1. Furthermore, overexpressed PKD1 could up regulate, whereas PKD1 antisense could knock down TRPV1 content in DRG through posttranscriptional regulation manner. We concluded that PKD1 in DRG, through interaction with TRPV1, is involved in developing and maintaining inflammatory heat hypersensitivity.

Keywords: Protein kinase D1 (PKD1); Transient receptor potential V1 (TRPV1); Inflammatory heat hypersensitivity; Gene delivery; Intrathecal injection

1. Introduction

Protein kinase D1 (PKD1), also known as protein kinase Cμ, is a recently described serine/threonine protein kinase with unique structural, enzymological, and

* Corresponding author. Tel.: +86 10 82801119; fax: +86 10 82801119.
E-mail address: wangy66@bjmu.edu.cn (Y. Wang).
[1] These authors contributed equally to this work.

0304-3959/$34.00
doi:10.1016/j.pain.2007.10.025

regulatory properties that differ from those of the PKC family members [16,32]. The most distinct characteristics of PKD1 are the presence of a catalytic domain distantly related to Ca^{2+}-regulated kinases, a pleckstrin homology domain within the regulatory region, and a highly hydrophobic stretch of amino acids in its N-terminal region.

PKD1 appears to be an important regulator of intracellular signaling pathways. It has been implicated in the regulation of a variety of cellular functions, including NFκB-mediated gene expression [29,30], Na^+/H^+ antiport activity [9], Golgi organization and function [7,13] and protein transport [21]. However, almost all the studies of PKD1 function involved only non-neuronal cells and most depended on the overexpression of exogenous PKD1. Little is known about the physiological function of PKD1 in the nervous system, especially at the animal level.

The vanilloid receptor type 1 (VR1), that is transient receptor potential V1 (TRPV1), is a vanilloid gated, nonselective cationic channel that belongs to the transient receptor potential (TRP) channel superfamily [3]. TRPV1 is expressed on small-diameter neurons within sensory ganglia and accounts for the highly selective action of vanilloids as excitatory agents for nociceptors. Moreover, TRPV1 is an integrator of nociceptive stimuli and plays a pivotal role in acute inflammatory pain [3]. Our previous *in vitro* study showed that PKD1 could directly phosphorylate TRPV1 in its N-terminal region and enhance the function of TRPV1 in CHO cells stably transfected with TRPV1 [36]. These results suggest that PKD1 may play an important role in inflammatory pain and that TRPV1 may function as a molecular target of PKD1 in inflammatory pain.

In the present study we sought to elucidate the involvement of PKD1 in pain modulation and explored the role of the interaction between PKD1 and TRPV1 in the rat inflammatory heat hypersensitivity.

2. Materials and methods

2.1. Experimental animals

Male Sprague–Dawley rats weighing 210–300 g were used in all experiments. Animals were housed in white plastic cages with solid bottoms covered with wood shavings under a 12 h light/dark cycle (lights on at 8:00 A.M.). Food and water were available *ad libitum*. All behavioral testings were done between 10:00 A.M. and 4:00 P.M. The animal use committee of the Peking University Health Science Center approved the protocols for all of our experiments.

2.2. Induction of inflammation

Unilateral inflammation was induced by subcutaneous injection of 100 μl CFA (Sigma, St. Louis, MO, USA) into the plantar surface of the left hind paw [11]. Naïve rats without CFA injection were designated as the control group. All animals (control and CFA-injected) received brief ether anesthesia in a fume hood and were equally handled. CFA injection produced localized swelling characterized by erythema, edema and hypersensitivity, the animals still exhibited normal grooming behavior and weight gain over the course of the experiments, as previously shown [11].

2.3. Assessment of hypersensitivity

A behavioral response involving a nociceptive flexion reflex elicited by thermal stimulation of the plantar surface of a hind paw was used as a measure of hypersensitivity during the course of inflammation. Animals were tested based on the thermal stimulus paradigm of Hargreaves et al. [8], using a Plantar Analgesia Instrument from Institute of Biomedical Engineering, Chinese Academy of Medical Science and Peking Union Medical College (Tianjin, China) which measures the paw withdrawal latency (PWL) from a radiant heat source directed at the core of the plantar surface of the hind paw. Before testing, animals were allowed to acclimatize to the testing environment for 1 h in a dedicated room. The radiant heat source was an infrared lamp, which was adjusted to result in baseline latencies of 12–15 s with a cut-off latency of 30 s, so as to avoid tissue damage. Four trials were conducted on each hind paw with consecutive trials separated by an interval of 5 min. The experimenter was blinded to all test paradigms. Because of considerable variability in the first latency measurement, three four-trial PWL measurements were averaged and the mean value was used to determine the PWL in the left and the right hind paws. This testing method allowed for side-to-side comparisons of inflamed and non-inflamed hind paws within test subjects.

Mechanical allodynia was tested by Von Frey filaments (Stoelting, USA) [5]. The paw withdrawal threshold was calculated using the up–down method.

Spontaneous Pain Latency was recorded by the period from CFA injection to the appearance of pain behaviors such as stamping and licking feet.

Experiments testing the effects of PKD1 in DRGs on PWL and on peripheral inflammation reaction were performed in the same groups of rats for optimal determination of possible correlations among these parameters.

2.4. Inclined-plane test

The rat was placed crosswise to the long axis of an inclined plane. The initial angle of the inclined plane was 50°. The angle was then adjusted in 5° increments. The maximum angle of the plane on which the rat maintained its body position for 5 s without falling was determined according to the method reported by Rivlin and Tator [24,25].

2.5. Subcloning of PKD1/PKCμ and mutagenesis of PKD1/PKCμ

The human PKD1 cDNA cloned in pbluescript SK (±) vector was provided by Dr. K. Pfizenmaier (Institute of Cell Biology and Immunology, University of Stuttgart, Germany). To generate the green fluorescent protein (GFP) fusion construct,

the human PKD1 was amplified by PCR and subcloned into the XhoI–MluI site of a pEGFP-N1 vector (Clontech, Mountain View, CA), and was then modified by inserting a MluI linker into the plasmid digested with SmaI.

The kinase inactive mutant (D727A) of human PKD1 was prepared by mutating an aspartate residue in the 727 position to alanine in the pEGFP-N1-PKD1 plasmid. Mutagenesis was performed with the QuickChange Site-directed mutagenesis kit (Stratagene, La Jolla, CA, USA). The mutation was confirmed by sequencing performed by the DNA minicore, Center for Cancer Research, NCI, NIH (Bethesda, MD, USA).

2.6. Intrathecal injection of PKD1 antisense-, sense-oligonucleotide and PKD1 expression vector

Male Sprague–Dawley rats weighing 180–220 g were anesthetized with chlorohydrate (0.4 g/kg i.p.). Implantation of i.t. cannulas was performed following the method of Storkson et al. [28]. PE-10 polyethylene catheters (o.d. 0.61 mm) were implanted between the L5 and L6 vertebrae under anesthesia to reach the lumber enlargement of the spinal cord. The outer part of the catheter was plugged and fixed onto the skin on closure of the wound. I.t. injection was made 5 d post surgical procedure. The PKD1 antisense-, sense-*oligonucleotide*, and GFP-PKD1 expression vectors were injected via the catheter in a volume of 10 and 40 μl, respectively, followed by 10 μl of normal saline (NS) for flushing. The injections took place over 5 min. After an injection, the needle remained in situ for 2 min before being withdrawn.

Phosphorothioate-modified oligonucleotides were purchased from Invitrogen (Carlsbad, CA). The antisense sequence used was 5′-ATG GAC CGG AGG GGC GCT CAT-3′ for PKD1 based on the start codon (ATG) plus the 15 additional downstream bases in the human PKD1 sequence. The sequences of sense and missense were 5′-ATG AGC GCC CCT CCG GTC-3′ and GCA GCA CAT CGC ATC GAC-3′, respectively. Oligonucleotide (20 μg) was diluted in 10 μl NS, and was then injected i.t. into groups of rats once a day for 4 d before measurement of responses.

In order to transfect the GFP vector, GFP-PKD1, GFP dominant negative PKD1 (GFP-DN-PKD1) and vehicle control, oligonucleotide–Lipofectamine 2000 complexes were prepared as follows: 10 μg of oligonucleotide was diluted in 10 μl of NS and gently mixed. Lipofectamine 2000 (20 μl) was added to 10 μl of NS and mixed gently. After 5 min incubation at room temperature, the diluted oligonucleotide was mixed with the diluted Lipofectamine 2000 by adding Lipofectamine 2000 solution into DNA solution and incubated for 20 min at room temperature to allow the oligonucleotide–Lipofectamine 2000 complexes to form. The mixture was then injected intrathecally as previously described.

2.7. Immunofluorescence

Adult male Sprague–Dawley rats were anesthetized with 0.4 g/kg chlorohydrate and transcardially perfused with saline, followed by 4% paraformaldehyde (in PBS). DRGs were removed, post-fixed in 4% paraformaldehyde for 4 h, treated with 30% sucrose (in PBS) for 24 h, and then embedded in Tissue-Tek OCT. Cryosections (8 μm) were cut and stored at −20 °C. Mounted DRG sections were allowed to thaw to room temperature. Indirect immunofluorescence was used to detect PKD1 and TRPV1 expression after CFA treatment. For analyses of co-localization of TRPV1 and PKD1 in DRG tissues, we used dual-labeling immunofluorescence. Donkey serum or goat serum was used for blocking for 6 h, at which time the antibody to TRPV1 (goat, Santa Cruz Biotechnology, 1:50) or PKD1 (rabbit, Santa Cruz Biotechnology, CA, USA, 1:200) was incubated for 48 h. FITC and Texas Red conjugated second antibodies were used. The stained sections were examined with a Leica fluorescence microscope (Nussloch, Germany) and a Leica TCS 4D confocal microscope using an omnichrome air-cooled helium/neon laser tuned to produce beams at 488 and 568 nm.

2.8. Tissue collection and immunoblot analysis

At 0, 2, 6 h and 1 d after CFA, animals were killed by decapitation and exsanguination, DRGs (L4 to L5) were removed as previously described [10]. The left half of the DRG (ipsilateral) corresponded to the inflamed paw and the right half of the DRG (contralateral) corresponded to the non-inflamed hind paw. L4/5 DRG was immediately homogenized in ice-chilled lysis buffer (50 mM Tris, pH 7.4, 150 mM NaCl, 1.5 mM $MgCl_2$, 10% glycerol, 1% Triton X-100, 5 mM EGTA, 0.5 μg/ml leupeptin, 1 mM PMSF, 1 mM Na_3VO_4, 10 mM NaF, proteinase inhibitor cocktail). The homogenates were centrifuged at 12,000*g* for 5 min at 4 °C to yield the total protein extract in the supernate. The concentration of protein was measured with a BCA assay kit (Pierce Biotechnology, Rockford, IL, USA). Equal amounts of samples (50 μg) were denatured and subjected to SDS–PAGE using 10% running gels and transferred to nitrocellulose membranes (Bio-Rad Laboratories, Hercules, CA, USA). The nitrocellulose membranes were blocked with 5% dry milk in TBST (50 mM Tris–HCl, pH 7.5, 150 mM NaCl, and 0.05% Tween 20) for 1 h at room temperature and incubated with the primary antibody, rabbit polyclonal anti-PKD1 (Santa Cruz Biotechnology, CA, USA, 1:1000), rabbit polyclonal anti-TRPV1 (Calbiochem, pc-420, 1:100), rabbit polyclonal anti-phospho-PKD1 (Ser744/748) (Cell signaling, #2054, 1:100), and anti-β-actin (Sigma, St. Louis, MO, USA. A5316, 1:2000 or 1:1000) overnight at 4 °C. Specific reactive bands were detected using a goat anti-rabbit or goat anti-mouse antibody conjugated to horseradish peroxidase (Zymed, USA), and the immunoreactive bands were visualized by the Western Blotting Luminol Reagent Kit (Santa Cruz Biotechnology, CA, USA). The intensities of the bands were quantified and the results are presented as relative values. In Deglycosylation assay, lysates from DRGs were treated with peptide-*N*-glycosidase F (New England Biolabs) for 1 h at 37 °C and subjected to SDS–PAGE.

2.9. Membrane (particulate) preparation and Western blot analysis of PKD1

L4/5 DRGs samples from individual rats were separately homogenized in ice-cold buffer A [50 mM Tris–HCl, pH 7.5, 0.25 M NaCl, 10 mM EDTA, 0.5% NP-40, 20 mM/ml leupeptin, 1 mM phenylmethylsulfonyl fluoride, and 4 mM NaF]. After being rotated at 4 °C for 1 h, the lysates were centrifuged at 500*g* at 4 °C for 15 min to remove cellular debris and then

centrifuged for 1 h at 25,000*g* at 4 °C. The supernatant constituted the cytosolic PKD1 preparation. The pellet was rinsed twice in the same buffer, re-suspended by a brief 30 s re-homogenization in buffer A containing 1% Triton X-100, and incubated on ice for 30 min with intermittent mixing. The extract was then centrifuged at 25,000*g* for 1 h with the supernatant constituting the membrane-associated (or particulate) PKD1 preparation. Then equal amounts of membrane protein (50 μg) were denatured and subjected to SDS–PAGE and analyzed by Western blotting.

2.10. Co-immunoprecipitation between TRPV1 and PKD1 in rat DRG

Rats were killed by decapitation under chlorohydrate (0.4 g/kg i.p.) anesthesia. The spinal columns were removed aseptically, and dorsal root ganglia from all levels or peripheral terminals were dissected out and homogenized in lysis buffer as above. After being rotated at 4 °C for 1 h, the lysates were centrifuged at 12,000 rpm at 4 °C for 15 min to remove cellular debris. The supernatant was incubated with either 5 μl of anti-PKD1 (1:100) polyclonal antibody, anti-TRPV1 polyclonal antibody or non-immune rabbit or goat IgG at 4 °C for 3 h. Protein A–Sepharose CL-4B resin (Santa Cruz Biotechnology, CA, USA) was added to the samples and the incubation was continued for a further 12 h, after which samples were washed six times with TBS, 0.1% Triton X-100. Separated proteins were fractionated on SDS polyacrylamide gels and subjected to Western blotting. The transferred proteins were detected sequentially using a polyclonal goat anti-rabbit PKD1 antibody and a rabbit anti-goat TRPV1 antibody on the same blot. Horseradish peroxidase-conjugated secondary antibodies and ECL (Santa Cruz Biotechnology, CA, USA) were used to visualize bands. For multiple detections with different antibodies, blots were first stripped in a solution of 62.5 mM Tris–HCl, pH 7.5, 20 mM dithiothreitol, and 1% SDS for 20–30 min at 50 °C and washed twice for 15 min with TBS, 0.1% Tween 20, followed by blocking and incubation with a new primary antibody.

2.11. Detection of mRNA by real time PCR

We performed real-time quantitative RT-PCR for PKD1 (XM_234108) and TRPV1 (NM_031982) mRNA (PKD1-s: 5′-CCGTCACGATCCTGCCTCTG-3′, PKD1-a: 5′-AGCC TTCTCCTTCTCACTCCAC-3′; rat TRPV1-s: 5′-TGGTGG AGGTGGCAGATAACAC-3′, rat TRPV1-a: 5′-GCCCATT CGGTGAACTTCCTG-3′). RNAs were isolated from DRGs of rats and reverse-transcribed into cDNAs by using a cDNA synthesis kit from Fermentans (RevertAid™ First strand cDNA Synthesis Kit, #k1622). The quality of cDNA was detected by running a regular PCR of house-keeping gene, 18s (rat-18S-s: 5′-CGGCTACCACATCCAAGGAA-3′, rat-18s-a: 5′-GCTGGAATTACCGCGGCT-3′) for 40 cycles at 95 °C for 15 s, 57 °C for 20 s and 72 °C for 20 s, and followed separating in ethidium bromide containing agarose gels. PCR machine is PTC-225 Peltier Thermal cycler (MJ Research Inc., Waltham, Massachusetts). Quantitative PCR machine is Rotor-Gene RG-3000 Real-Time Thermal Cycler (Corbett Research, Sydney, Australia). The real-time PCR was performed using a SYBR premix kit (TOYOBO, QPK-201T), and running it for 40 cycles at 95 °C for 15 s, 57 °C for 20 s and 72 °C for 20 s. The PCR efficiency was also examined by serially diluting the template cDNA and the melting curve data were collected to check the PCR specificity and proper negative controls were included in each assay. Relative quantification for any given gene, expressed as fold variation over control, was calculated from the determination of the difference between the Ct of the test gene and that of the calibrator gene (18S RNA). Ct values used were the means of triplicate replicates. Experiments were repeated at least five times.

2.12. Dissociation of dorsal root ganglion neurons

Sprague–Dawley male rats (250 g) treated as described above were decapitated under ethyl ether anesthesia. The vertebral column was rapidly removed and dissected in ice-cold Dulbecco's modified Eagle's medium (DMEM) (Invitrogen). L4-L6 dorsal root ganglions were picked out and treated with collagenase (type IA, 3 mg/ml, Sigma) and trypsin (type I, 1 mg/ml, Sigma) in DMEM at 36.8 °C for 25 min with 5% CO_2 and 95% O_2. After incubation, the ganglia were washed 5 times with the standard electrophysiology external solution and then gently triturated using fine fired-polished Pasteur pipettes. The dissociated DRG neurons were plated onto 3.5 cm culture dishes and incubated at 4 °C for at least 2 h before electrophysiological recording.

2.13. Electrophysiology

Whole-cell patch clamp recording of DRG neurons was performed at room temperature (20–22 °C) with an EPC-9 amplifier (Heka Electronic, Germany). Microelectrodes (Glass GG-17, O.D. = 1.5mm) were fabricated with a P801-A puller (Narishige, Japan), and those with a resistance of 2–6 MΩ were used. Stimulation protocols and data acquisition were controlled by the software Pulse+Pulsefit 8.5 (Heka Electronic, Germany). Series resistance was routinely compensated (70–80%), and data were sampled at 20 kHz and low-passed at 5 kHz.

For recording the capsaicin-evoked current, cells were held at their resting potential. The external solution contained (in mM): 140 NaCl, 5 KCl, 1 $MgCl_2$, 2.5 $CaCl_2$, 10 HEPES, 10 D-glucose, pH 7.4, with an osmolarity of 320 mosM. The patch pipette was back filled with the intracellular solution (in mM): 140 KCl, 1 $MgCl_2$, 0.5 $CaCl_2$, 5 EGTA (ethylene glycol-bis (β-aminoethyl ether)-*N*,*N*,*N*′,*N*′-tetraacetate), 3 Na_2ATP, 10 HEPES (*N*-(2-hydroxyethyl)piperazine-*N*′-(2-ethanesulfonic acid)), pH 7.2, with an osmolality of 300 mosM. Under fluorescence microscopy, the visible small-diameter DRG neurons (<25 μm) at an excitation wavelength of 488 nm were recorded. All the drugs were dissolved in external solution and applied to the DRG neurons with a gravity-driven perfusion system. Exchange of the bath solution was complete within 100 ms.

2.14. Image analysis

For DRG analysis, five randomly selected sections from the L4 and L5 DRG of normal rats were used. All immunoreactive positive profiles in a section were outlined, creating an artificial overlay. The average intensity and feret area of each object identified by the overlay was then measured automatically by

MetaMorph software. Proportions of neurons labeled for PKD1 per total immmunoreactive positive neurons and the average intensity of PKD1 immunoreactivity were calculated according to the size of the cell body.

2.15. Statistical analysis

Data are presented as means ± SEM. Differences between groups were compared using either the Student's *t*-test or an analysis of variance (ANOVA). The criterion for statistical significance was $P < 0.05$. Electrophysiological data acquired with Pulse software were analyzed with SigmaPlot 2000 or Igor pro 4.0., and statistical comparisons were made using the unpaired two-tail *t*-test and Fisher exact test; differences were considered statistically significant when $P < 0.05$.

3. Results

3.1. PKD1 is expressed in pain-sensing neurons

Although PKD1 is expressed extensively in various tissues and cells, it has been reported that little or no PKD1 is present in primary sensory neurons [4,18]. It has been well demonstrated that tissue distribution and subcellular localization are both closely correlated with protein kinase function. We therefore evaluated PKD1 expression in DRG using RT-PCR and Western blot and determined the cellular distribution of PKD1 by immunostaining methods. The blocking peptide to PKD1 antibody was used to insure specificity. Non-immune rabbit IgG was used as a negative control.

RT-PCR for DRG revealed a band at the appropriate size for full length PKD1 (Fig. 1A). Furthermore, PKD1 was prominently detected in the central, the peripheral terminal and the cell body of DRGs, but little in paw skin, by Western blot analysis (Fig. 1B), and pre-absorption of the antibody with blocking peptide confirmed its specificity (Fig. 1B). Furthermore, we used fluorescence microscopy of frozen sections to examine the cellular distribution of PKD1 in DRG. It showed that PKD1 was present in the large-, medium- and small-sized neurons, and PKD1 distribution in medium- and small-sized neurons is much more frequent than that in large-sized ones, but the expression intensity did not show large discrepancy (Fig. 1C and D). Moreover, PKD1 largely co-localized with TRPV1 (a specific marker for nociceptive C fibers) in DRG neurons

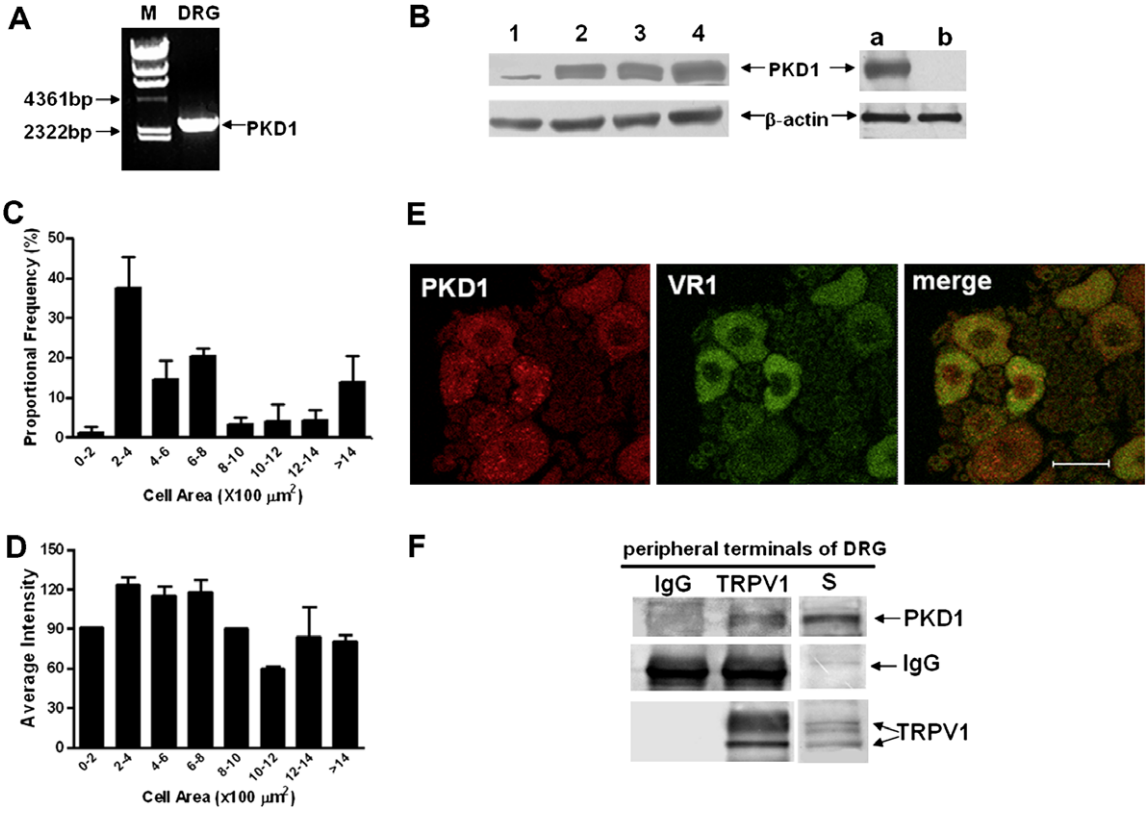

Fig. 1. Expression and distribution of PKD1 in the DRG. (A) RT-PCR results showed full length PKD1 mRNA in the DRG. M, marker; DRG, dorsal root ganglion. (B) PKD1 in DRG detected by Western blot. 1, paw skin; 2, central terminals of DRG; 3, DRG cell body; 4, peripheral terminals of DRG; a, DRG lysate, blotted with antibody of PKD1; b, DRG lysate, preincubation with blocking peptide for PKD1. (C) Size-frequency distribution of PKD1-immunoreactive neurons. (D) Average intensity of PKD1 immunoreactivity in DRG neurons of different sizes. (E) Double immunostaining of PKD1 (red) and VR1 (green) in DRG. Scale bar, 40 μm. (F) PKD1 was precipitated by TRPV1 antibody in peripheral terminals of DRG, Normal goat IgG instead of TRPV1 antibody was used as control, S, supernatant.

(Fig. 1E). Normal rabbit or goat IgG was used in place of primary antibody and produced nonspecific staining in DRG sections (data not shown). Besides, PKD1 can interact with TRPV1 in the peripheral terminal of DRG, where TRPV1 is abundant (Fig. 1F).

Taken together, both PKD1 mRNA and protein were present in DRG at the L4/5 level in the normal adult rats. Moreover, PKD1 prominently distributed in the medium- and small-sized neurons of DRGs at the L4/5 level and was localized in TRPV1-positive neurons, which contribute to pain hypersensitivity. We therefore proposed that PKD1 played a role in pain modulation. To further explore this possibility, we evaluated the involvement of PKD1 in the model of inflammatory pain induced by CFA.

3.2. Dynamic changes of PKD1 activity in DRGs during inflammation induced by CFA

We used the model of inflammatory pain induced by injection of CFA as described previously [11]. CFA (100 μl) was injected under the surface of the left hind paw where it caused local inflammation. Heat hypersensitivity and mechanical allodynia were induced at 2 and 6 h after CFA injection, peaked at 1 d, and maintained a relatively stable level for up to one week following the CFA injection.

We evaluated the time course of PKD1 expression in the cell membrane and cytoplasm of DRGs at the L4/5 level by Western blot after CFA injection. PKD1 in ipsilateral DRGs translocated to cytoplamic membranes at 2 and 6 h and recovered at 1 d after the onset of inflammation (Fig. 2A and Fig. 2B). According to the quantitative analysis, PKD1 in cytoplasmic membrane significantly increased more than 4-fold at 2 and 6 h after inflammation. However, PKD1 in cytoplasm decreased to half of the control level at 2 and 6 h after inflammation (Fig. 2C and E).

As reported, PKD1 can be activated by transphosphorylation at Ser744/748 [23,34]. We therefore determined the phosphorylation status of PKD1 in the DRGs at different time points after CFA injection using phosphorylation specific PKD1 antibody. Western blot and quantitative analyses showed that phos-

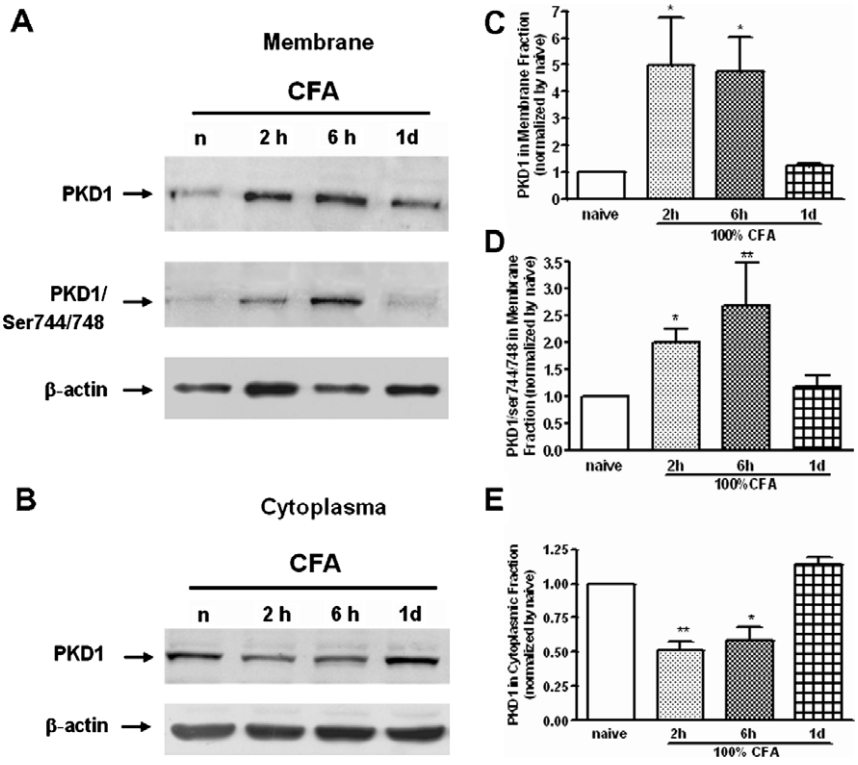

Fig. 2. Dynamic changes of PKD1 protein level in the DRG during inflammation induced by CFA. (A) First panel: the time course of PKD1 expression in the ipsilateral DRG membrane following CFA injection. Second panel: the phosphorylation status of PKD1 in the DRG at different time points after CFA injection. Western blot analyses showed that phosphorylation of PKD1 from the membrane fraction at Ser744/748 increased significantly at 2 and 6 h, then returned to the baseline level one day after CFA treatment. (B) The time course of PKD1 expression in the ipsilateral DRG cytoplasm following CFA injection. (C and D) Quantification of PKD1 (C) and phosphorylation of PKD1 at Ser744/748 (D) from membrane fraction in DRG after inflammation. Each column refers to means ± SEM and represents three separate experiments. Data were normalized by naïve control and analysis of ANOVA followed by Dunnett's Multiple Comparison Test. $^{*}P < 0.05$, $^{**}P < 0.01$, as compared with naïve rats, $n = 4$. (E) Quantification of PKD1 from cytoplasm fraction in DRG following CFA. Each column refers to means ± SEM and represents three separate experiments. Data were normalized by naïve control and analysis of ANOVA followed by Dunnett's Multiple Comparison Test. $^{*}P < 0.05$, $^{**}P < 0.01$, as compared with naïve rats, $n = 4$.

phorylation of PKD1 at Ser744/748 increased significantly more than 2-fold at 2 and 6 h, and then returned to the baseline level at 1 d after CFA treatment in the membrane fraction (Fig. 2A and D). This is consistent with the fact that PKD1 always translocates to the membrane once it has been activated. β-Actin was used as loading control.

3.3. PKD1 was involved in the initiation of CFA-induced heat hypersensitivity

Since PKD1 was activated at 2 and 6 h after CFA treatment, we investigated whether PKD1 activation at the early stage of CFA-induced inflammation contributed to the induction of pain hypersensitivity. Because there is no specific inhibitor of PKD1 enzymatic activity, we used two alternative approaches to assess the effect on CFA-induced pain behaviors of blocking PKD1 activity. We used a PKD1 antisense ODN that could specifically knockdown the expression of PKD1; we also used a dominant negative PKD1 that could specifically inhibit the activity of PKD1. Conversely, we evaluated the effect on CFA-induced pain behaviors on enhancing the function of PKD1 through overexpression of wild-type PKD1.

We injected normal saline (NS), PKD1 missense oligonucleotide, PKD1 sense oligonucleotide and PKD1 antisense oligonucleotide once a day for 4 d before CFA injection. We then measured protein level of PKD1 by Western blot in DRGs at 6 h after CFA injection. The PKD1 protein level in DRG was significantly decreased to about 50% in rats treated with PKD1 antisense oligonucleotide compared with PKD1 missense

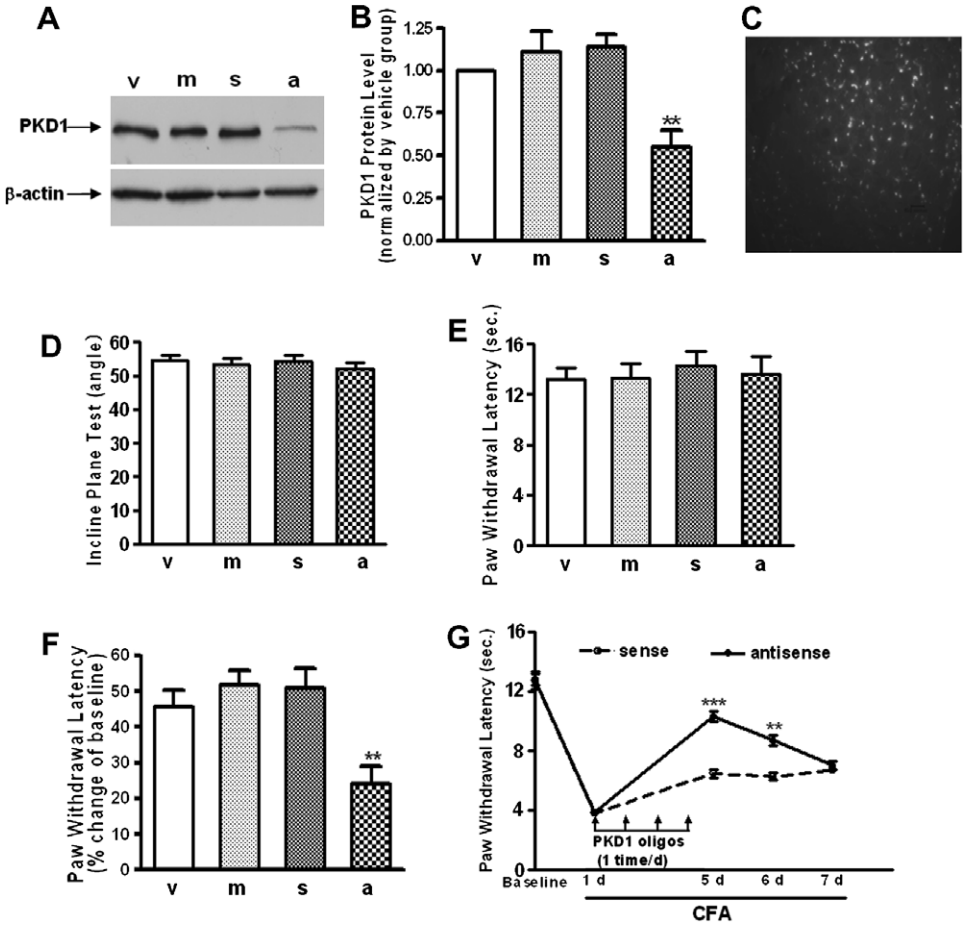

Fig. 3. Effects of PKD1 antisense on PKD1 protein level in DRG and the nociceptive responses following CFA injection. (A) Effect of intrathecal injection of PKD1 antisense on PKD1 expression in total cell lysate at 6 h after CFA injection. v, vehicle; m, missense of PKD1; s, sense of PKD1; a, antisense of PKD1. (B) Quantification of PKD1 expression in DRG illustrated similar changes as showed in A. The results were expressed as means ± SEM in three rats per group for three separate experiments. Data were normalized to the vehicle control and analyzed by an ANOVA followed by a Newman–Keuls test. $^{**}P < 0.01$, as compared to the other groups. (C) Distribution of PKD1 antisense ODN in DRG detected by fluorescein isothiocyanate (FITC)-labeled oligonucleotide. (D and E) Intrathecal injection of PKD1 antisense did not affect the motor function of rats detected by the inclined-plane test (D) and had no effect on basal paw withdrawal latency (E). (F) Effect of PKD1 antisense on heat hypersensitivity 6 h following 50% CFA injection. Data were normalized to the baseline value before CFA injection and analyzed by an ANOVA followed by a Newman–Keuls test. $^{**}P < 0.01$, as compared with other groups, $n = 8$–9. (G) Effect of PKD1 antisense on the maintenance of heat hypersensitivity following CFA injection. Data were analyzed by an unpaired t-test at the individual time points and across the three experiments. $^{***}P < 0.001$, $^{**}P < 0.01$ as compared with sense group, $n = 9$–12. oligos:oligonucleotides.

oligonucleotide and sense oligonucleotide at 6 h after CFA injection (Fig. 3A and B).

To better understand the basis for the effect of the PKD1 antisense oligonucleotide in the DRGs, we determined the distribution of PKD1 antisense oligonucleotide in DRGs using fluorescein isothiocyanate (FITC)-labeled oligonucleotide. Corresponding to the biological effects of PKD1 antisense oligonucleotide, fluorescence from the PKD1 antisense oligonucleotide mainly accumulated in DRG (Fig. 3C).

We next measured the behavior of rats treated with the various oligonucleotide constructs. We found that in the animals not treated with CFA neither the motor function detected by the inclined plane test [25] nor the basal nociceptive response detected by PWL differed between the PKD1 antisense group and the PKD1 missense or PKD1 sense groups (Fig. 3D and E). In contrast, PKD1 antisense could affect the PWL in animals treated with CFA. In these experiments, 50% CFA (diluted by incomplete Freund′s adjuvant) was used to avoid spontaneous pain behavior. The results revealed that heat hypersensitivity was attenuated significantly in rats treated with PKD1 antisense oligonucleotide at 6 h following CFA injection, compared with other groups ($P < 0.05$) (Fig. 3F), but mechanical allodynia did not differ among these groups (data not shown). Taken together, the results suggest that intrathecal injection of PKD1 antisense oligonucleotide suppresses the PKD1 protein level in DRG and significantly attenuates CFA-induced thermal hypersensitivity in the rats.

To further confirm the involvement of PKD1 in the initiation of CFA-induced inflammatory pains we delivered exogenous genes into DRG and evaluated their effect on nociceptive responses. At 6 d after intrathecal injection of GFP, GFP-PKD1 and GFP-DN-PKD1 genes with Lipofectamine 2000, there was strong fluorescence in the DRGs compared to the Lipofectamine 2000 alone control (Fig. 4A). No significant differences

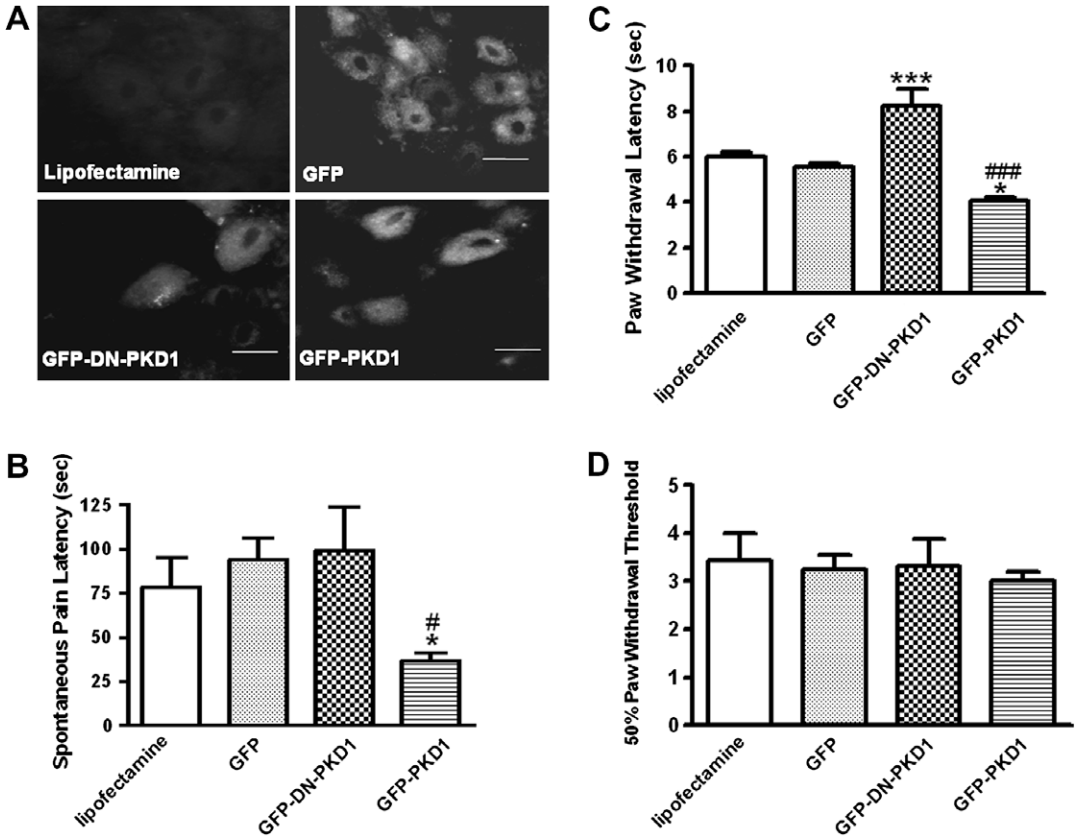

Fig. 4. Effects of delivery of exogenous genes into DRG on nociceptive responses. (A) A stronger signal is shown in DRG following delivery of GFP, GFP-PKD1, and GFP-DN-PKD1 genes compared with following treatment with lipofectamine 2000 alone. Scale bar, 40 μm. Data represent three independent experiments. (B) The spontaneous pain latency was decreased by delivery of GFP-PKD1 relative to that of the other genes. Data are expressed as means ± SEM and represent three separate experiments. Data were analyzed by an ANOVA followed by a Newman–Keuls Multiple Comparison Test. $^{*}P < 0.05$, as compared with GFP group, $^{\#}P < 0.05$, as compared with GFP-DN-PKD1 group, $n = 6$–8. (C) Delivery of the GFP-PKD1 gene enhanced while the GFP-DN-PKD1 gene attenuated heat hypersensitivity 6 h following CFA treatments. Data were expressed as mean ± SEM and represented three separate experiments. Data were analyzed by an ANOVA followed by a Newman–Keuls Multiple Comparison Test. $^{*}P < 0.05$, $^{***}P < 0.001$, as compared with GFP group, $^{\#\#\#}P < 0.001$, as compared with GFP-DN-PKD1 group, $n = 6$–8. (D) Delivery of exogenous genes did not affect mechanical allodynia detected by von Frey hair. $n = 6$–8. Data represented three independent experiments. GFP, green fluorescence protein; GFP-PKD1, PKD1-fused green fluorescence protein; GFP-DN-PKD1, dominant negative mutant (D727A) of PKD1-fused green fluorescence protein.

among these groups were detected in basal nociceptive response to radiant heat or in motor function as measured by the inclined plane test (data not shown). However, spontaneous pain latency (the period from CFA injection to the appearance of pain behaviors such as stamping and licking feet) was decreased by delivery of the GFP-PKD1 gene compared with other groups (Fig. 4B). Moreover, overexpression of PKD1 significantly decreased while overexpression of GFP-DN-PKD1 significantly increased PWL ($P < 0.05$ and < 0.01 compared with the GFP group, respectively) (Fig. 4C). We also assessed mechanical allodynia by the von Frey hair test. No significant differences were observed between the different treatment groups (Fig. 4D).

In summary, all the results indicated that suppression of PKD1 by antisense or delivery of GFP-DN-PKD1 gene significantly decreased heat hypersensitivity following CFA injection. Conversely, the increase of PKD1 activity by delivery of the PKD1 gene enhanced heat hypersensitivity.

3.4. PKD1 was involved in the maintenance of heat hypersensitivity induced by CFA

The above data show that PKD1 was involved in the induction of hypersensitivity. Next, we explored whether PKD1 participated in the maintenance of heat hypersensitivity induced by CFA. At 24 h after CFA injection, rats of each group were intrathecally injected with NS, PKD1 sense oligonucleotide, PKD1 missense oligonucleotide, or PKD1 antisense oligonucleotide, once a day for four successive days at a dose of 20 μg/day. The nociceptive responses were then detected by von Frey hair and radiant heat stimuli. The results indicated that the rats treated with PKD1 antisense oligonucleotide had significantly increased PWL compared with the rats treated with the PKD1 sense ($P < 0.01$) (Fig. 3G). However, for the von Frey hair test, the paw withdrawal threshold was not increased in either testing group.

3.5. Interaction of PKD1 and TRPV1 contributed to heat hypersensitivity induced by CFA

All the results discussed thus far demonstrate that PKD1 is involved in heat hypersensitivity induced by CFA. However, as a protein kinase, PKD1 cannot directly participate in synaptic transduction. What might be the targets of PKD1 that participate in heat hypersensitivity induced by CFA? Our previous studies demonstrated that PKD1 directly phosphorylated the N-terminal fragment of TRPV1 and enhanced the activity of TRPV1 [36]. Therefore, we investigated whether PKD1 could interact with TRPV1 to participate in heat hypersensitivity induced by CFA.

Fig. 1E shows that PKD1 and TRPV1 were co-localized in the cytoplasm of the medium- and small-sized neurons in the normal rat DRG. In order to prove the interaction between PKD1 and TRPV1 following CFA injection, we carried out co-immunoprecipitation experiments. Interaction between PKD1 and TRPV1 was detected only at 6 h after CFA injection (Fig. 5A), although PKD1 was precipitated in all specimens. Likewise, using precipitation with TRPV1 antibody, we found that the binding between PKD1 and TRPV1 was much stronger at 6 h than that at the other time points (Fig. 5B). Furthermore, immunofluorescence confirmed that PKD1 and TRPV1 appeared co-localized on neuronal membranes in the DRG neurons 6 h following CFA injection (Fig. 5C).

To test the effect of PKD1 on the function of TRPV1 in vivo, we conducted electrophysiological experiments with acutely dissociated DRG neurons. The results show that the climax inward current of positively responding neurons by different dose of capsaicin was also higher in the PKD1 overexpression rats than that in the dominant negative PKD1 overexpression ones (Fig. 6), which indicates more sensitivity of TRPV1 in the PKD1 overexpression rats. The responsive cell number to 0.5 μM capsaicin in the PKD1 overexpression rats was also greater than that in the dominant negative PKD1 ones (Fig. 7). The higher climax inward current for the PKD1 overexpression rats suggests a role of PKD1 in TRPV1 functional modulation through either phosphorylation of TRPV1 or increase of TRPV1 content.

In order to elucidate the possible mechanism of PKD1 involvement in the maintenance of heat hypersensitivity, we detected the time course of TRPV1 protein level in DRG following CFA treatment and also detected TRPV1 protein level in DRG of rat subjected to either antisense interference or gene delivery. The results indicate that TRPV1 content increased 2 d following CFA treatment (Fig. 8A). Interestingly, as can been seen in Fig. 8A, TRPV1 displayed two bands in the DRG samples of rats detected by Western blot analysis. A previous study suggested that the down band is the monomer of TRPV1 and the up band is the glycosylated monomer of TRPV1 in CHO-TRPV1 cell [17]. In order to confirm whether the up band is the glycosylated TRPV1, we treated the DRG samples from inflammatory pain rat with peptide-*N*-glycosidase F, which confirmed that the up band was the glycosylated monomer of TRPV1 (Fig. 8A). Furthermore, we found that both the monomer and glycosylated TRPV1 were down regulated in DRG neurons of rats injected PKD1 antisense, with reduced PKD1 protein level (Fig. 8B, 8C and 8D). However, TRPV1 mRNA detected by real-time PCR was not affected, while PKD1 mRNA was largely suppressed by i.t. PKD1 antisense 2 d after inflammation (Fig. 8E and F). On the other hand, overexpression of PKD1 increased the

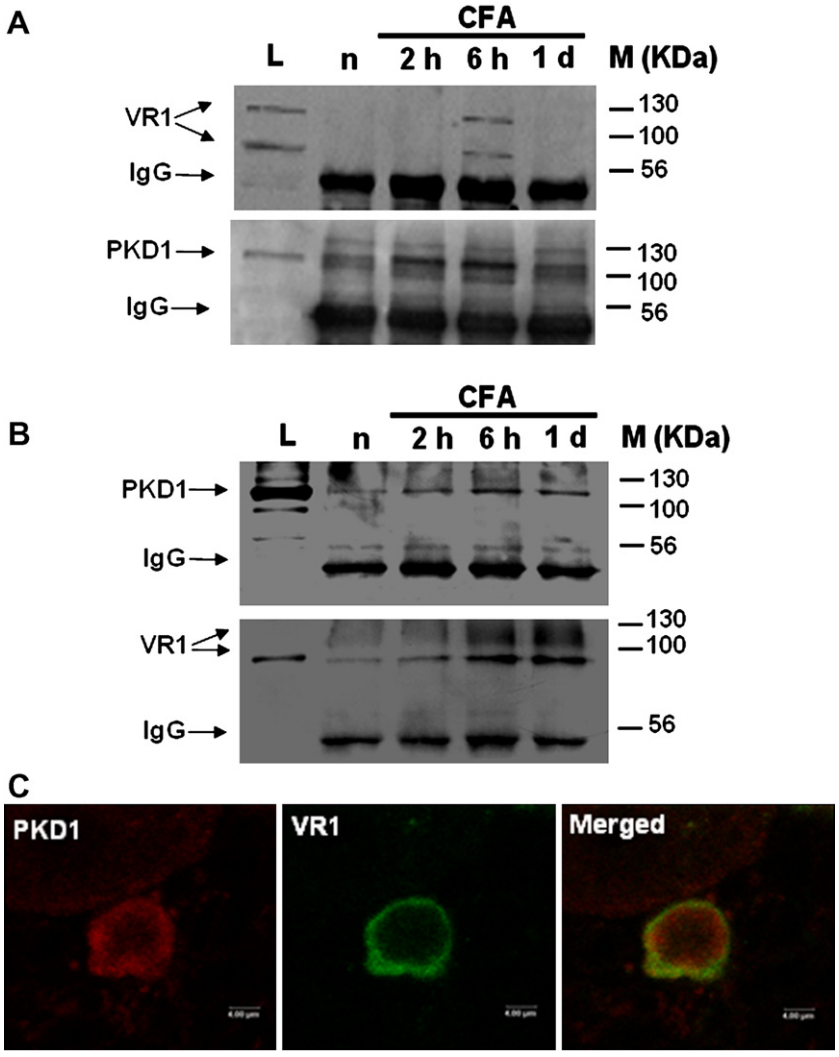

Fig. 5. Immunoprecipitation and co-localization between PKD1 and VR1 in DRG. (A) VR1 was immunoprecipitated by PKD1 antibody at 6 h following CFA injection. IgG was used as loading control. L, DRG lysate; n, naïve. Data represent three independent experiments. (B) PKD1 was immunoprecipitated by VR1 antibody. IgG was used as loading control. L, DRG lysate; n, naïve. Data represent three independent experiments. (C) VR1 translocated to the surface membrane and co-localized with PKD1 in small DRG neurons 6 h after CFA injection. Visualization was by confocal microscopy. Scale bar, 40 μm. Data represent three separate experiments.

protein level of TRPV1 (Fig. 8G and H), suggesting that transient activation of PKD1 following CFA injection may induce TRPV1 up regulation in DRG neurons through a posttranscriptional manner, this may serve as one of the mechanisms contributing to the maintenance of heat hypersensitivity.

4. Discussion

The above data provide evidence for the interaction of PKD1 with TRPV1 in heat hypersensitivity following inflammation. PKD1 mRNA and protein were expressed in adult rat DRG neurons. Peripheral inflammation induced PKD1 activation in the DRG and PKD1 contributed to heat hypersensitivity through the functional modulation of TRPV1. To our knowledge this is the first report showing the activation pattern and function of PKD1 in the nervous system in response to noxious stimulation.

Firstly, we found PKD1 were expressed in adult rat DRG neurons, which is inconsistent with the study of Cesare et al. The discrepancy may be because of the antibody. They used the monoclonal antibody [4]. And we confirmed the PKD1 expression in DRG by RT-PCR and Western blot. Since the activation pattern of PKD1 in response to inflammation presents special feature, which was fast and transient. PKD1 activation started at 30 min or earlier, reached a peak at 2 and 6 h, and returned to a baseline level within 1 d post inflammation, suggesting it may be involved in the development of pain hypersensitivity. It is reported PKD1 can be activated by novel PKCs, in which, PKCε is responsible for heat hyperalgesia [4,18]. But other candidate for PKC-independent PKD1 activation needs further study.

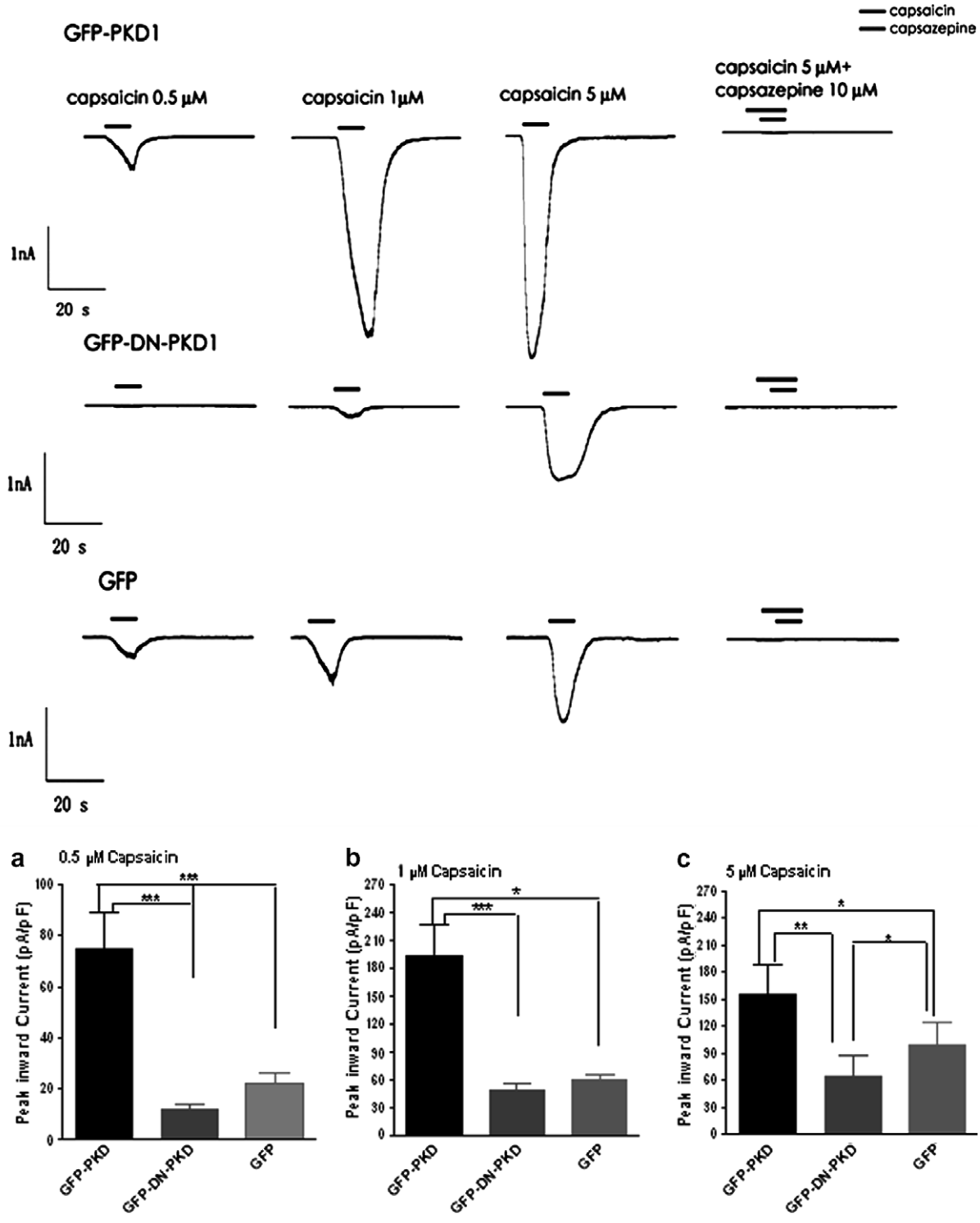

Fig. 6. Effects of capsaicin on small DRG neurons of different groups transfected with GFP constructs by electrophysiological experiments with acutely dissociated DRG neurons. The curves indicate the typical dose-dependent capsaicin-evoked current on DRG neurons of different groups. The capsaicin-evoked current was completely blocked by 10 μM capsazepine. a, b and c: The evoked capsaicin current density (pA/pF) of different groups. Unpaired two-tail *t*-tests were used. $^{*}P < 0.05$, $^{**}P < 0.01$ and $^{***}P < 0.001$ indicate significant differences from GFP vector group.

Through the gene delivery with Lipofectamine 2000, we investigated if PKD1 was involved in inflammation-induced heat hypersensitivity. The non-viral plasmid vector delivery with Lipofectamine 2000 had advantages of reproducibility and a lack of side effects (nearly no immune response or toxic effects). In recent reports, this method has been used successfully to transfer foreign genes into the DRG and spinal cord

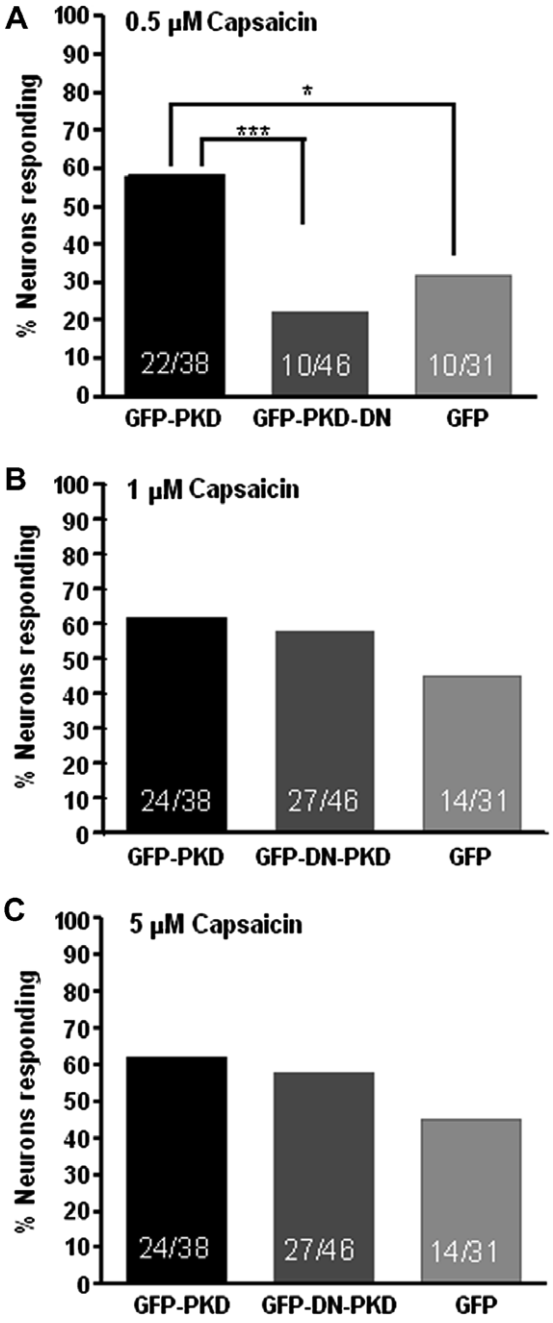

Fig. 7. Effects of capsaicin on small DRG neurons of different groups transfected with GFP constructs. Neurons were held at resting potential. Different concentrations of capsaicin were administrated to each neuron from low to high at 2 min intervals. Ten micrometer capsaicin evoked an inward current in more than 50% of the neurons. The neurons with a current above 40 pA were counted. (A) The responding proportion to 0.5 μM capsaicin on neurons from different treatment groups. Groups were compared using Fisher exact test, $^{*}P < 0.05$, and $^{***}P < 0.001$ indicate significant differences from GFP vector group. (B) Effect of 1 μM capsaicin on neurons of different treatment groups. (C) Effect of 5 μM capsaicin on neurons of different treatment groups.

by intrathecal injection [22,35,38,39]. It was also well applied in our groups [38], and the efficiency of the method is similar to delivery by adeno-associated virus type 2 [35]. Interestingly, PKD1 was involved in the induction of heat hypersensitivity rather than of mechanical allodynia. TRPV1 functioned as a target of PKD1 in the early stages of inflammatory pain, and PKD1 potentiated the function of TRPV1 through direct phosphorylation of TRPV1 [36].

Moreover, PKD1 was also involved in the maintenance of heat hypersensitivity. Our current results show that knockdown of PKD1 via post-inflammation injection of antisense could suppress heat hyperalgesia, the content of TRPV1 in DRG neurons was simultaneously decreased. And the opposite effect was produced by overexpression of PKD1, suggesting that transient activation of PKD1 may increase TRPV1 protein level in DRG neurons, which may serve as one of the mechanisms contributing to the maintenance of heat hypersensitivity.

In agreement with several previous studies [15,27,31,33], we did not detect any increase in TRPV1 mRNA levels in the DRG after induction of peripheral inflammation (data not shown). Neither did we find a decrease in TRPV1 mRNA after intrathecal PKD1 antisense treatment. However, both inflammation and overexpressed PKD1 increased the expression of TRPV1 protein levels in the DRG, suggesting that PKD1 may be involved in the posttranscriptional regulation of TRPV1 through downstream signals in the pain process. For example, the p38 signaling pathway, fully activated in the inflammatory process [15], is a downstream target of PKD1 [20], and it has been reported to be involved in the increase of TRPV1 protein levels in primary sensory neurons and in maintaining heat hypersensitivity after inflammation [15]. Thus, p38 may function as the target of PKD1 to induce TRPV1 up regulation through posttranscriptional regulation. Additional studies will be necessary to evaluate these various possibilities.

Several studies have reported that TRPV1 can be glycosylated in the pore loop region in heterologously expressed system or in the ostensibly more native context of the dorsal root ganglion-derived F-11 cell line [12,17,26], at a site that occurs near the beginning of the predicted pore loop. A subsequent study showed that the channel mutated at the glycosylation site N604 exhibited much less maximal current induced by capsaicin (I_{max} ~2600 pA versus 4200 pA for the wild-type channel), although greater sensitivity to the TRPV1 agonist, capsaicin (EC50 0.3 μM versus 1.4 μM for the wild-type channel). In addition, the capsaicin-induced current conducted by the mutant channel was less sensitive to the inhibitor, capsazepine [37], which indicates that *N*-glycosylation of the TRPV1 modulates the capsaicin/capsazepine binding capability of the receptor and is involved in the regulation of pH-sensitivity of capsaicin-induced responses. Consistent with this observation, we found glycosylated TRPV1 expressed in DRG neurons in both control and inflammatory rats. Moreover, the glycosylated form of TRPV1 increased

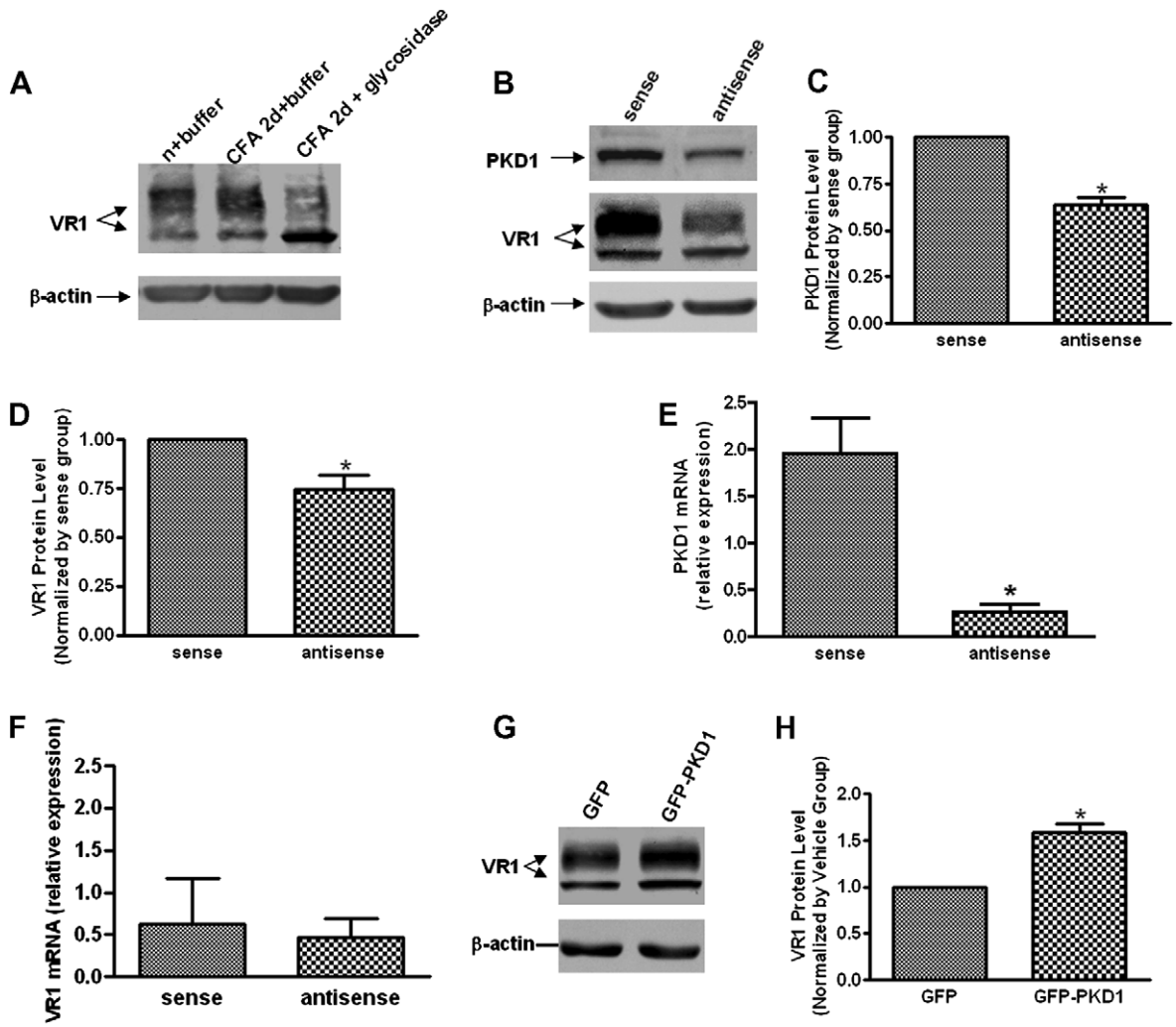

Fig. 8. PKD1 affected VR1 expression level in DRG following CFA injection. (A) TRPV1, both monomer and up band, was increased in DRG 2 d following CFA injection. Glycosidase treatment decreased the up band but increased the monomer. n, naïve; buffer, Glycosidase reaction buffer. Data represent three independent experiments. (B) PKD1 antisense down regulated TRPV1 content as detected by Western blot. (C and D) Quantification of PKD1 (C) and TRPV1 (D) contents in DRG illustrated similar changes as shown in (B). The results were expressed as means ± SEM in three rats per group for three separate experiments. Data were normalized to the sense group and analyzed by paired *t*-test. $^{*}P < 0.05$, as compared to the sense group. (E and F) Quantification of PKD1 (E) and TRPV1 mRNA (F) detected by real time PCR. $^{*}P < 0.05$, as compared to the sense group. (G) Overexpression of PKD1 could up regulate TRPV1 content as detected by Western blot. Data represent three independent experiments. (H) Quantification of TRPV1 content in DRG illustrated similar changes as shown in (G). The results were expressed as mean ± SEM in three rats per group for three separate experiments. Data were normalized to the GFP control and analyzed by paired *t*-test. $^{*}P < 0.05$, as compared to the GFP group.

in DRG neurons from inflammatory rats, which could be regulated by PKD1 activity, suggesting that TRPV1 glycosylation will be modulated by certain condition such as hypersensitivity and PKD1 may functioned as one of the modulator. The role of glycosylated TRPV1 in pain signal transduction remains to be further investigated.

It is well known that there are many intracellular signals other than TRPV1 involved in inflammatory pain, and PKD1 thus might have other molecular targets which regulate the pain process. One potential target is the ERK signal pathway, which is fully activated in the inflammatory process [14] and is a downstream target of PKD1 [2]. Another potential target is NFκB, which is also a downstream target of PKD1, and was reported to be involved in hypersensitivity of inflammatory and pathological pain rat [19]. Since the activation of NFκB leads to up regulation of NFκB responsive genes such as proinflammatory genes, potentiated hypersensitivity, and inflammation, NFκB activation may contribute to the maintenance of heat hypersensitivity induced by activation of PKD1. The $P_2X_{(7)}$ receptor is a new target in peripheral inflammatory nociception, and the $P_2X_{(7)}$ receptor signal transduction pathway could activate PKD1 and induce PKD1 phosphorylation [1]. It was reported recently that in mice

lacking $P_2X(_7)$, inflammatory (in an adjuvant-induced model) as well as neuropathic (in a partial nerve ligation model) hypersensitivity in response to both mechanical and thermal stimuli is completely absent, although normal nociceptive processing is preserved [6]. Therefore, the dissection of the potential multiple contributions of PKD1 to inflammatory hypersensitivity may be quite involved.

In summary, we demonstrated that PKD1 plays an important role in the development and maintenance of CFA-induced inflammatory heat hypersensitivity at the peripheral level (DRG). One of the mechanisms of PKD1 involvement in nociceptive signal pathway was through potentiating TRPV1 function (induction of heat hypersensitivity) and increasing TRPV1 protein level (maintenance of heat hypersensitivity).

Acknowledgments

This work was supported by a grant from the National Natural Science Foundation of China (30330026); the grant of Outstanding Young Teacher of Higher Academic School to Y.W. from the Ministry of Education of China [2001-182]. The research was supported in part by the intramural program of the NIH, National Cancer Institute, Center for Cancer Research.

References

[1] Bradford MD, Soltoff SP. P_2X_7 receptors activate protein kinase D and p42/p44 mitogen-activated protein kinase (MAPK) downstream of protein kinase C. J Biol Chem 2002;366:745–55.

[2] Brandlin I, Hubner S, Eiseler T, Martinez-Moya M, Horschinek A, Hausser A, et al. Protein kinase C (PKC)eta-mediated PKC mu activation modulates ERK and JNK signal pathways. J Biol Chem 2002;277:6490–6.

[3] Caterina MJ, Schumacher MA, Tominaga M, Rosen TA, Levine JD, Julius D. The capsaicin receptor: a heat-activated ion channel in the pain pathway. Nature 1997;389:816–24.

[4] Cesare P, Dekker LV, Sardini A, Parker PJ, McNaughton PA. Specific involvement of PKC-epsilon in sensitization of the neuronal response to painful heat. Neuron 1999;23:617–24.

[5] Chaplan SR, Bach FW, Pogrel JW, Chung JM, Yaksh TL. Quantitative assessment of tactile allodynia in the rat paw. J Neurosci Methods 1994;53:55–63.

[6] Chessell IP, Hatcher JP, Bountra C, Michel AD, Hughes JP, Green P, et al. Disruption of the P_2X_7 purinoceptor gene abolishes chronic inflammatory and neuropathic pain. Pain 2005;114:386–96.

[7] Diaz Anel AM, Malhotra V. PKCeta is required for beta1gamma2/beta3gamma2- and PKD-mediated transport to the cell surface and the organization of the Golgi apparatus. J Cell Biol 2005;169:83–91.

[8] Hargreaves KM, Troullos ES, Dionn RA, Schmidt EA, Schafer SC, Joris JL. Bradykinin is increased during acute and chronic inflammation: therapeutic implications. Clin Pharmacol Ther 1988;44:613–21.

[9] Haworth RS, Sinnett-Smith J, Rozengurt E, Avkiran M. Protein kinase D inhibits plasma membrane Na(+)/H(+) exchanger activity. Am J Physiol 1999;277:1202–9.

[10] Igwe OJ, Filla MB. Regulation of phosphatidylinositide transduction system in the rat spinal cord during aging. Neuroscience 1995;69:1239–51.

[11] Igwe OJ, Ning L. Regulation of the second-messenger systems in the rat spinal cord during prolonged peripheral inflammation. Pain 1994;58:63–75.

[12] Jahnel R, Dreger M, Gillen C, Bender O, Kurreck J, Hucho F. Biochemical characterization of the vanilloid receptor 1 expressed in a dorsal root ganglia derived cell line. Eur J Biochem 2001;268:5489–96.

[13] Jamora C, Van Lint J, Laudenslager J, Vandenheede JR, Faulkner DJ, Yamanouye N, et al. Gbetagamma-mediated regulation of Golgi organization is through the direct activation of protein kinase D. Cell 1999;98:59–68.

[14] Ji R-R, Baba H, Brenner GJ, Woolf CJ. Nociceptive-specific activation of ERK in spinal neurons contributes to pain hypersensitivity. Nat neurosci 1999;2:1114–9.

[15] Ji R-R, Samad TA, Jin S-X, Schmoll R, Woolf CJ. p38 MAPK activation by NGF in primary sensory neurons after inflammation increases TRPV1 levels and maintains heat hyperalgesia. Neuron 2002;36:57–68.

[16] Johannes FJ, Prestle J, Eis S, Oberhagemann P, Pfizenmaier K. PKCμ is a novel, atypical member of the protein kinase C family. J Biol Chem 1994;269:6140–8.

[17] Kedei N, Szabo T, Lile JD, Treanor JJ, Olah Z, Iadarola MJ, et al. Analysis of the Native Quaternary Structure of Vanilloid Receptor 1. J Biol Chem 2001;276:28613–9.

[18] Khasar SG, Lin YH, Martin A, Dadgar J, McMahon T, Wang D, et al. A novel nociceptor signaling pathway revealed in protein kinase C epsilon mutant mice. Neuron 1999;24:253–60.

[19] Lee KM, Kang BS, Lee HL, Son SJ, Hwang SH, Kim DS, et al. Spinal NF-κB activation induces COX-2 upregulation and contributes to inflammatory pain hypersensitivity. Eur J Neurosci 2004;19:3375–81.

[20] Lemonnier J, Ghayor C, Guicheux J, Caverzasio J. Protein kinase C-independent activation of protein kinase D is involved in BMP-2-induced activation of stress mitogen-activated protein kinases JNK and p38 and osteoblastic cell differentiation. J Biol Chem 2004;279:259–64.

[21] Liljedahl M, Maeda Y, Colanzi A, Ayala I, Van Lint J, Malhotra V. Protein kinase D regulates the fission of cell surface destined transport carriers from the trans-Golgi network. Cell 2001;104:409–20.

[22] Luo MC, Zhang DQ, Ma SW, Huang YY, Shuster SJ, Porreca F, et al. An efficient intrathecal delivery of small interfering RNA to the spinal cord and peripheral neurons. Mol Pain 2005.

[23] Matthews SA, Rozengurt E, Cantrell D. Characterization of serine 916 as an in vivo autophosphorylation site for protein kinase D/Protein kinase C mu. J Biol Chem 1999;274:26543–9.

[24] Rivlin AS, Tator CH. Regional spinal cord blood flow in rats after severe cord trauma. J Neurosurg 1978;49:844–953.

[25] Rivlin AS, Tator CH. Objective clinical assessment of motor function after experimental spinal cord injury in the rat. J Neurosurg 1977;47:577–81.

[26] Rosenbaum T, Awaya M, Gordon SE. Subunit modification and association in VR1 ion channels. BMC Neurosci 2002:3–4.

[27] Sanchez JF, Krause JE, Cortright DN. The distribution and regulation of vanilloid receptor VR1 and VR1 5′ splice variant RNA expression in rat. Neuroscience 2001;107:373–81.

[28] Storkson RV, Kjorsvik A, Tjolsen A, Hole A. Lumbar catheterization of the spinal subarachnoid space in the rat. J Neurosci Methods 1996;65:167–72.

[29] Storz P, Doppler H, Toker A. Protein kinase Cδ selectively regulates protein kinase D-dependent activation of NF-κB in oxidative stress signaling. Mol Cell Biol 2004;24:2614–26.

[30] Storz P, Toker A. Protein kinase D mediates a stress-induced NF-κB activation and survival pathway. EMBO J 2003;22:109–20.

[31] Tohda C, Sasaki M, Konemura T, Sasamura T, Itoh M, Kuraishi Y. Axonal transport of VR1 capsaicin receptor mRNA in primary afferents and its participation in inflammationinduced increase in capsaicin sensitivity. J Neurosci 2001;76:1628–35.
[32] Valverde AM, Sinnett-Smith J, Van Lint J, Rozengurt E. Molecular cloning and characterization of protein kinase D: a target for diacylglycerol and phorbol esters with a distinctive catalytic domain. Proc Natl Acad Sci USA 1994;91:8572–6.
[33] Voilley N, de Weille J, Mamet J, Lazdunski M. Nonsteroid anti-inflammatory drugs inhibit both the activity and the inflammation-induced expression of acid-sensing ion channels in nociceptors. J Neurosci 2001;21:8026–33.
[34] Waldron RT, Rey O, Iglesias T, Tugal T, Cantrell D, Rozengurt E. Activation loop Ser^{744} and Ser^{748} in protein kinase D aretransphosphorylated in vivo. J Biol Chem 2001;276:32606–15.
[35] Wang X, Wang C, Zeng J, Xu X, Hwang PYK, Yee W-C, et al. Gene transfer to dorsal root ganglia by intrathecal injection: effects on regeneration of peripheral nerves. Mol ther 2005;12:314–20.
[36] Wang Y, Kedei N, Wang M, Wang QJ, Huppler AR, Toth A, et al. Interaction between PKCμ and the vanilloid receptor type 1. J Biol Chem 2004;279:53674–82.
[37] Wirkner K, Hognestad H, Jahnel R, Hucho F, Illes P. Characterization of rat transient receptor potential vanilloid 1 receptors lacking the *N*-glycosylation site N604. Neuroreport 2005;16: 997–1001.
[38] Yang YR, He Y, Zhang Y, Li Y, Li Y, Han Y, Zhu H, et al. Activation of cyclin-dependent kinase 5 (Cdk5) in primary sensory and dorsal horn neurons by peripheral inflammation contributes to heat hyperalgesia. Pain 2007;127: 109–20.
[39] Yao M-Z, Gu J-F, Wang J-H, Sun L-Y, Lang M-F, Liu J, et al. Interleukin-2 gene therapy of chronic neuropathic pain. Neuroscience 2002;112:409–16.